

1 **Exploring the role of the metabolite-sensing receptor GPR109a in diabetic**
2 **nephropathy**

3 Matthew Snelson^{1*}, Sih Min Tan¹, Gavin C. Higgins¹, Runa Lindblom¹, Melinda T.
4 Coughlan^{1,2}

5 **Affiliations:**

6 ¹Department of Diabetes, Central Clinical School, Alfred Medical Research and
7 Education Precinct, Monash University, Melbourne, Victoria, Australia.

8 ²Baker Heart and Diabetes Institute, Melbourne, Australia.

9 *matthew.snelson@monash.edu
10

11 **Corresponding Author:**

12 Dr Matthew Snelson

13 matthew.snelson@monash.edu

14 Level 5, Alfred Centre, 99 Commercial Road, Melbourne 3004 VIC, Australia
15

16 **Keywords**

17 GPR109a; resistant starch; diabetic nephropathy; intestinal permeability; dietary fibre.
18

19 **Running title**

20 GPR109a, type 1 diabetes and kidney injury
21
22
23

24 **Abstract**

25

26 Alterations in gut homeostasis may contribute to the progression of diabetic
27 nephropathy. There has been recent attention on the renoprotective effects of
28 metabolite-sensing receptors in chronic renal injury, including the G-protein-coupled-
29 receptor (GPR)109a, which ligates the short chain fatty acid butyrate. However, the role
30 of GPR109a in the development of diabetic nephropathy, a milieu of diminished
31 microbiome-derived metabolites, has not yet been determined. This study aimed to
32 assess the effects of insufficient GPR109a signalling via genetic deletion of GPR109a
33 on the development of renal injury in diabetic nephropathy. *Gpr109a*^{-/-} mice or their
34 wildtype littermates (*Gpr109a*^{+/+}) were rendered diabetic with streptozotocin (STZ).
35 Mice received a control diet or an isocaloric high fiber diet (12.5% resistant starch) for
36 24 weeks and gastrointestinal permeability and renal injury were determined. Diabetes
37 was associated with increased albuminuria, glomerulosclerosis and inflammation. In
38 comparison, *Gpr109a*^{-/-} mice with diabetes did not show an altered renal phenotype.
39 Resistant starch supplementation did not afford protection from renal injury in diabetic
40 nephropathy. Whilst diabetes was associated with alterations in intestinal morphology,
41 intestinal permeability assessed *in vivo* using the FITC-dextran test was unaltered.
42 GPR109a deletion did not worsen gastrointestinal permeability. Further, 12.5% resistant
43 starch supplementation, at physiological concentrations, had no effect on intestinal
44 permeability or morphology. These studies indicate that GPR109a does not play a
45 critical role in intestinal homeostasis in a model of type 1 diabetes or in the development
46 of diabetic nephropathy.

47

48 **Introduction**

49
50 Diabetic nephropathy is a major microvascular complication of diabetes, occurring in up
51 to 30% of patients with type 1 diabetes [1]. Concomitant with the rise in diabetes and
52 obesity, the prevalence of diabetic nephropathy has been increasing rapidly, with
53 diabetic nephropathy now the leading cause of end stage renal disease worldwide [1].
54 Despite optimal conventional management with pharmacological inhibition of the renin
55 angiotensin system (RAS), glycemic and blood pressure control, a significant proportion
56 of patients with DKD still progress over time to end stage renal failure. Thus, there is an
57 urgent need for the identification of new therapeutic options to help limit the progression
58 of this disease.

59 Recently there has been an increasing interest in the diet-gut-kidney axis,
60 whereby elements derived from the diet alter the composition of the gut microbiota and
61 production of microbial metabolites which induce effects at extra-intestinal sites,
62 including the kidneys [2, 3]. It has been noted that patients with diabetes [4] and end
63 stage renal disease [5, 6] have a contraction in the bacterial taxa that produce beneficial
64 short chain fatty acids (SCFAs). Furthermore, during end stage renal disease, there is
65 an increase in intestinal permeability and subsequent inflammation [7]. SCFAs act via
66 local metabolite-sensing receptors in order to reduce intestinal permeability and
67 inflammation [8, 9]. The use of dietary therapies that directly target the gut microbiota to
68 increase SCFA production, including probiotics and prebiotics, have been recently
69 considered as potential adjunct interventions to limit injury in diabetic nephropathy [10].

70 Butyrate acts as a ligand for the G-protein-coupled-receptor (GPR)109a,
71 decreasing intestinal inflammation and promoting gut epithelial barrier integrity, thus

72 GPR109a activation is considered to be protective [11]. A recent study showed that
73 GPR109a modulated the renoprotective effect of butyrate on adriamycin-induced
74 nephropathy [3], however, the role of GPR109a in the development of diabetic
75 nephropathy has not been determined.

76 This study aimed to assess the effects of insufficient GPR109a signalling via
77 genetic deletion of GPR109a on the development of renal injury in diabetic
78 nephropathy. *Gpr109a*^{-/-} mice or their wildtype littermates (*Gpr109a*^{+/+}) were rendered
79 diabetic with streptozotocin (STZ). Mice received a control diet or an isocaloric, high
80 fiber diet containing 12.5% resistant starch for 24 weeks and gastrointestinal
81 permeability and renal injury were determined.

82 **Materials and Methods**

83

84 **Animals**

85 Male mice homozygous for a deletion in the GPR109a receptor (*Gpr109a*^{-/-}), were
86 obtained from Professor Charles Mackay (Monash University, Victoria, Australia) [11],
87 and crossbred with wildtype (WT) C57BL6/J mice purchased from The Jackson
88 Laboratory to produce heterozygous mice, which were then mated to produce *Gpr109a*^{-/-}
89 *-/-* knockout (KO) mice and littermate WT controls. Mice were housed in a climate-
90 controlled animal facility that had a fixed 12-hour light and 12-hour dark cycle and
91 provided with *ad libitum* access to water and chow. All study protocols were conducted
92 in accordance to the principles and guidelines devised by the Alfred Medical Research
93 & Education Precinct Animal Ethics Committee (AMREP AEC) under the guidelines laid
94 down by the National Health and Medical Research Council (NHMRC) of Australia and
95 had been approved by the AMREP AEC (E1487/2014/B).

96

97 **Induction of Diabetes**

98 Diabetes was induced at six weeks of age by five daily intraperitoneal injections of
99 streptozotocin (55 mg/kg Sigma Aldrich) in sodium citrate buffer. Diabetes was
100 confirmed by a glycated haemoglobin (GHb) greater than 8%. Two mice failed to meet
101 this cutoff and were excluded from any further analysis. Of those diabetic mice that
102 were included in the analysis, the mean GHb was 11.7% (median 11.9%).

103

104 **Diet Intervention**

105 Since previous studies exploring the role of resistant starch (RS) on the development of
106 renal injury have used supraphysiological doses over a short period of time, we sought
107 to supplement a dose of resistant starch that could be more reasonably expected to be
108 consumed by people (25% HAMS Hi maize 1043, equivalent to 12.5% RS) over a
109 longer time frame (24 weeks). From six weeks of age, mice received either a custom-
110 made control diet (CON) or a high fiber diet supplemented with resistant starch
111 prepared by Speciality Feeds (Perth, Western Australia, Australia). Both of these semi-
112 pure diets were formulated based on a modified AIN93G growth diet for rodents. These
113 diets were isocaloric, had equivalent protein, provided as 20% g/g casein, and fat,
114 provided as 7% g/g canola oil. Each diet contained 5% g/g sucrose, 13.2% g/g
115 dextrinised starch and 7.4% g/g cellulose. A resistant starch supplemented diet (SF15-
116 015) was formulated with 25% g/g Hi-maize 1043, whilst the CON diet (SF15-021)
117 contained an additional 20% g/g regular starch and 5% g/g cellulose in order to maintain
118 caloric equivalency between diets. Hi-maize 1043, an RS2 starch prepared from high
119 amylose maize starch (HAMS) which contains 50% resistant starch [12], was provided
120 as a raw ingredient by Ingredion (Westchester, IL, USA). Mice received these
121 experimental diets *ad libitum* for 24 weeks.

122

123 **Tissue collection**

124 At the end of the study period, mice were anaesthetised by an intraperitoneal injection
125 of 100 mg/kg body weight sodium pentobarbitone (Euthatal; Sigma-Aldrich, Castle Hill,
126 Australia) followed by cardiac exsanguination. Following cardiac exsanguination, blood
127 was immediately centrifuged at 6000 rpm for 6 minutes and plasma was snap frozen on
128 dry ice and stored at -80°C. Kidney sections were fixed in neutral buffered formalin
129 (10% v/v). The gastrointestinal tract was dissected and the mesentery removed.
130 Sections of the gastrointestinal tract were weighed and length measured. The ileum was
131 flushed with chilled phosphate buffered saline. Ileum sections were fixed in
132 paraformaldehyde (4% v/v) for 24 hours before being transferred to 4% sucrose solution
133 and embedded in paraffin. Ileum sections were snap frozen in liquid nitrogen and stored
134 at -80°C, for ribonucleic acid (RNA) analysis.

135

136

137 **Glycated haemoglobin**

138 Glycated haemoglobin (GHb) was measured in blood collected at cull using a Cobas b
139 101 POC system (Roche Diagnostics, Forrenstrasse, Switzerland) according to the
140 manufacturer's instructions. The Cobas b 101 POC system has a detection range of
141 between 4-14%, with any sample with a GHb less than 4% designated as low and
142 samples with a GHb of greater than 14% designated high.

143

144 ***In Vivo* Intestinal Permeability Assay**

145 Intestinal permeability was assessed *in vivo* using the previously described dextran
146 FITC technique [13], during the week prior to cull. In brief, mice were fasted for a
147 minimum of four hours and received an oral gavage of a 125 mg/mL solution of dextran
148 FITC equivalent to 500 mg/kg body weight. After one hour, approximately 120 μ L was
149 collected from the tail vein using heparinised capillary tubes. Blood was centrifuged at
150 6000 rpm for 6 minutes, plasma collected and the fluorescence in plasma samples was
151 determined in relation to a standard dilutions set, using a fluorescence
152 spectrophotometer (BMG Labtech, Ortenberg, Germany) set to excitation 490nm,
153 emission 520nm. The intra- and interassay coefficients of variation were 3.2 and 8.9%,
154 respectively.

155

156 **Body Composition**

157 Fat mass and lean body mass were determined using a 4-in-1 EchoMRI body
158 composition analyser (Columbus Instruments, Columbus, OH, USA), which measures
159 fat mass, lean mass and total water content using nuclear magnetic resonance
160 relaxometry [14]. The weight of mice prior to being placed in the body composition
161 analyser was used for calculation of percentage fat and lean mass.

162

163 **Metabolic Caging, Urine and Plasma Analyses**

164 After 23 weeks of experimental diet, mice were housed individually in metabolic cages
165 (Iffa Credo, L'Arbresle, France) for 24 hours for urine collection and measurement of

166 urine output and food and water intake. The animals received *ad libitum* access to food
167 and water during this period. Urine was stored at -80°C until required for analyses.
168 Urinary albumin was determined using a mouse specific ELISA (Bethyl Laboratories,
169 Montgomery, TX, USA) according to the kit protocol. The intra- and interassay
170 coefficients of variation were 7.3 and 8.9%, respectively. Urinary monocyte
171 chemoattractant protein-1 (MCP-1) was measured using a commercially available
172 ELISA kit (R&D Systems, Minneapolis MN, USA) as per the kit protocol. The intra- and
173 interassay coefficients of variation were 2.8 and 4.0%, respectively. Blood urea nitrogen
174 was analysed using a commercially available colorimetric urea assay (Arbor Assays,
175 Ann Arbor, MI, USA) as per the kit protocol. The intra- and interassay coefficients of
176 variation were 4.5 and 3.9%, respectively. Plasma cystatin C was determined using a
177 commercially available ELISA from R&D Systems. The intra- and interassay coefficients
178 of variation were 3.8 and 8.3%, respectively

179

180 **Kidney and Ileum Histology**

181 Kidneys were fixed in 10% (v/v) neutral buffered formalin prior to embedding in paraffin.
182 Kidney sections (3 µm) were stained with periodic acid-Schiff (PAS) and assessed in a
183 semiquantitative manner, whereby a blinded researcher assessed the level of
184 glomerulosclerosis for each glomerulus and assigned an integer score of between 1 and
185 4, indicative of the level of severity of glomerulosclerosis. Twenty-five glomeruli were
186 scored per animal, and these scores were averaged to provide a glomerulosclerosis
187 score index (GSI) for each animal, as previously described [15]. Ileal sections were

188 fixed in 4% paraformaldehyde for 24 hours, followed by a transfer to 4% sucrose, and
189 subsequent embedding in paraffin. Ileal sections (5 μ m) were stained with haemotoxylin
190 and eosin (H&E) and images were captured using a brightfield microscope (Nikon
191 Eclipse-Ci; Nikon, Tokyo, Japan) coupled with a digital camera (Nikon DS-Fi3; Nikon,
192 Tokyo, Japan). Morphological measurements of villus height and crypt depth were
193 conducted using ImageJ (Version 1.52a). Villus height was measured from the topmost
194 point of the villus to the crypt transition, whilst the crypt depth was measured as the
195 invagination between two villi to the basement membrane.

196

197 **Quantitative RT-PCR**

198 RNA was isolated from snap frozen ileum sections using a phenol-chloroform extraction
199 method and used to synthesise cDNA, as previously described [15]. Gene expression of
200 zonulin and occludin was determined using TaqMan (Life Technologies) and SYBR
201 Green reagents (Applied Biosystems), respectively. Gene expression was normalised to
202 18S mRNA utilising the $\Delta\Delta$ Ct method and reported as fold change compared to WT
203 non-diabetic mice receiving the control diet.

204

205 **Statistical Analyses**

206 Data were analysed by two-way ANOVA with the Tukey posthoc test for multiple
207 comparisons. Analyses were performed using GraphPad Prism Version 7.01 (GraphPad

208 Software, La Jolle, CA, USA). Data are shown as mean \pm SEM. A value of $p < 0.05$ was
209 considered statistically significant.

210 **Results**

211 **Metabolic and Phenotypic parameters**

212 Consistent with the diabetic phenotype, mice with STZ-induced diabetes had increased
213 glycated haemoglobin and decreased body weight (Table 1). Diabetes was associated
214 with a decrease in relative fat mass and an increased lean mass and increased 24-hour
215 urine output and water intake (Table 1). Neither deletion of the GPR109a receptor nor
216 consumption of the high fiber (resistant starch) diet was associated with changes in
217 glycated haemoglobin, body weight or body composition. Diabetes was associated with
218 an increased liver weight and a decreased spleen weight (Table 1). Mice with diabetes
219 had an increase in small intestine length ($p < 0.001$, Fig 1A) caecum length ($p < 0.0001$,
220 Fig 1B), small intestine weight ($p < 0.0001$, Fig 1D), caecum weight ($p < 0.0001$, Fig 1E)
221 and colon weight ($p < 0.0001$, Fig 1F). Consumption of the fiber supplement led to an
222 increase in caecal weight and length in diabetic mice, but not in non-diabetic mice (Fig
223 1B, 1E). Resistant starch supplementation was also associated with an increase in
224 colon weight (Fig 1F).

225

226 **Renal Injury and Inflammation**

227 Diabetic mice exhibited the hallmarks of diabetic nephropathy, including albuminuria
228 ($p < 0.0001$, Fig 2A), increased blood urea nitrogen ($p < 0.0001$, Fig 2B), renal
229 hypertrophy ($p < 0.0001$, Fig 2C) and hyperfiltration ($p < 0.0001$, Fig 2D). Genetic ablation
230 of *Gpr109a* resulted in no change in the renal phenotype in diabetic mice (Fig 2A-D).

231 Likewise, the high fiber diet in the context of diabetes did not alter hallmarks of diabetic
232 nephropathy (Fig 2A-D). Diabetes was associated with an increase in the inflammatory
233 marker MCP-1, whilst there was no effect of either resistant starch supplementation or
234 deletion of *Gpr109a* ($p < 0.0001$, Fig 2E). Assessment of renal histology revealed an
235 overall increase in glomerulosclerosis in the diabetic setting, however, genetic ablation
236 of *GPR109a* or supplementation with the high fiber diet did not impact on renal
237 structural injury ($p < 0.0001$, Figure 3A & B).

238

239 **Intestinal Permeability and Morphology**

240 To determine whether *Gpr109a* deletion led to changes in intestinal morphology,
241 histology of the ileum was undertaken. Diabetes was associated with an overall
242 increase in villi height ($p < 0.0001$, Fig 4A & C) and a reduction in crypt depth ($p < 0.001$,
243 Fig 4B & C) in the ileum. In non-diabetic mice, deletion of *GPR109a* was associated
244 with a trend towards increased villi height ($p = 0.06$, Fig 4A). The high fiber diet led to a
245 trend towards an increase in villi height in non-diabetic wildtype and in *Gpr109a*^{-/-}
246 diabetic mice (Fig 4A). Despite these morphological changes in the ileum with diabetes,
247 diabetes did not induce any alteration in intestinal permeability, as measured by an *in*
248 *vivo* intestinal permeability procedure (dextran-FITC, Fig 4D) or as determined by gene
249 expression of the tight junction proteins occludin (*Ocln*, Fig 4E) or zonulin (*Tjp-1*) (Fig
250 4F).

251 Discussion

252 The current study explored the effects genetic deletion of the butyrate receptor,
253 GPR109a, had on the development of chronic renal injury in diabetic nephropathy. No
254 effect on the diabetic renal phenotype was observed with deletion of *Gpr109a*.
255 Surprisingly, there was no change in intestinal permeability or morphometry as a result
256 of *Gpr109a* deletion. Furthermore, a high fiber 12.5% resistant starch diet was not
257 effective in reducing renal injury in the setting of diabetes.

258 This is the first study to assess the effects of deletion of GPR109a on diabetic
259 nephropathy and these findings show that deletion of this receptor was not associated
260 with any change in renal injury in long term studies (24 weeks). Given the hypothesis
261 that renal injury would occur downstream of alterations in intestinal permeability and
262 there was no effect of *Gpr109a* deletion on *in vivo* assessment of intestinal permeability,
263 this should perhaps not come as a surprise finding. *In vitro*, *Gpr109a* knockdown inhibits
264 butyrate-induced increases in the tight junction protein Claudin-3, suggesting that
265 GPR109a may have a role in the integrity of the intestinal epithelial barrier [9]. However
266 *in vivo*, whilst deletion of GPR109a was associated with a trend towards an increase in
267 intestinal permeability in an induced food allergy model [16] there was no effect in
268 otherwise healthy mice [8], indicating that deletion of the GPR109a receptor alone is
269 insufficient to alter intestinal permeability. There is redundancy in the metabolite-
270 sensing GPCR family, with butyrate being recognised by GPR109a, GPR41 and GPR43
271 receptors. Indeed, it has been suggested that given this redundancy, single knockout
272 models are insufficient to fully elucidate the effects of these receptors, and that double
273 or triple knockout models are required [17].

274 Resistant starch is a type of dietary fibre that acts as a prebiotic. Numerous
275 studies have illustrated that supplementation with resistant starch is associated with an
276 increase in the microbial production of SCFAs, particularly butyrate [10]. A commonly
277 used source of resistant starch is high amylose maize starch (HAMS) and in an obese
278 model of diabetes, the Zucker diabetic fatty rat, six weeks of supplementation with a diet
279 containing 55% HAMS (Amylogel, equivalent to 20% resistant starch) was associated
280 with a reduction in albuminuria [18]. In addition, in the adenine-induced rat model of
281 chronic kidney disease, supplementation of 59% HAMS diet (Hi-maize 260, equivalent
282 to 27% resistant starch) for three weeks was associated with improvements in
283 creatinine clearance [19]. Conversely however, a study that supplemented a diet
284 containing 55% HAMS (Amylogel, equivalent to 20% resistant starch) for four weeks in
285 male Sprague-Dawley rats with streptozotocin-induced diabetes did not find any
286 renoprotective benefit with resistant starch supplementation [20]. Whilst these results
287 show promise, the concentrations of HAMS used in these studies are likely to be much
288 greater than could be reasonably expected to be consumed by people.

289 Since previous studies exploring the role of resistant starch on the development
290 of renal injury have used supraphysiological doses over a short period of time, we
291 sought to supplement a dose of resistant starch that could be more reasonably
292 expected to be consumed by people (25% HAMS Hi maize 1043, equivalent to 12.5%
293 resistant starch) over a longer time frame (24 weeks). In the present study, we
294 investigated the effects of resistant starch supplementation, at a dose of ~12.5%, on the
295 development of diabetic nephropathy in the STZ-induced diabetic mouse.

296 Supplementation of a high fiber resistant starch diet in such chronic studies was not
297 renoprotective.

298 A recent study showed that a renoprotective effect of butyrate on adriamycin-
299 induced nephropathy in short term studies [3]. In that study, intraperitoneal injection of
300 butyrate for 7 or 14 days in a model of adriamycin-induced nephropathy; and dietary
301 supplementation of a high fiber butyrylated resistant starch diet for four weeks prior to
302 adriamycin-induced nephropathy (preventative approach), showed that butyrate led to a
303 decreased urinary protein to creatinine ratio. Although no measures of intestinal
304 permeability were determined, that study shows promise for butyrate as a
305 renoprotective agent, at least in the acute setting, most likely attributable to acute
306 inflammation.

307 In conclusion, this study shows that long term resistant starch supplementation at
308 a dosage that would reasonably be expected to be consumed by humans, did not
309 alleviate albuminuria in the STZ-induced diabetes model. Whilst diabetes was
310 associated with alterations in intestinal morphology, there was no change in intestinal
311 permeability. It would be pertinent to consider resistant starch supplementation in other
312 rodent models of diabetes that may be more representative of the intestinal changes
313 that occur with diabetes in humans. Finally, this study indicates that GPR109a deletion
314 does not play a critical role in the development of diabetic nephropathy nor
315 gastrointestinal homeostasis.

316

317 **Acknowledgements**

318 The authors would like to thank the following people: Maryann Arnstein for technical
319 assistance, Professor Charles R. Mackay (Monash University) for the *GPR109a*^{-/-} mice,
320 Warren Potts from Specialty Feeds, Australia for the design and generation of the diets.
321 MS and RSJL were supported by scholarships from the Australian government
322 Research Training Program. GCH was supported by a postdoctoral fellowship from
323 JDRF. SMT is supported by a JDRF Advanced Postdoctoral Fellowship and MTC is
324 supported by a Career Development Award from the JDRF Type 1 Diabetes Clinical
325 Research Network, a special research initiative of the Australian Research Council.

326

327 **Declarations of interest**

328 None.

329 References

- 330 1. Alicic, R.Z., M.T. Rooney, and K.R. Tuttle, *Diabetic Kidney Disease: Challenges,*
331 *Progress, and Possibilities.* Clin J Am Soc Nephrol, 2017. **12**(12): p. 2032-2045.
- 332 2. Evenepoel, P., R. Poesen, and B. Meijers, *The gut-kidney axis.* Pediatr Nephrol,
333 2017. **32**(11): p. 2005-2014.
- 334 3. Felizardo, R.J.F., et al., *Gut microbial metabolite butyrate protects against*
335 *proteinuric kidney disease through epigenetic- and GPR109a-mediated*
336 *mechanisms.* FASEB J, 2019: p. fj201901080R.
- 337 4. Forslund, K., et al., *Disentangling type 2 diabetes and metformin treatment*
338 *signatures in the human gut microbiota.* Nature, 2015. **528**: p. 262.
- 339 5. Wong, J., et al., *Expansion of Urease- and Uricase-Containing, Indole- and p-*
340 *Cresol-Forming and Contraction of Short-Chain Fatty Acid-Producing Intestinal*
341 *Microbiota in ESRD.* American Journal of Nephrology, 2014. **39**(3): p. 230-237.
- 342 6. Jiang, S., et al., *Alteration of the gut microbiota in Chinese population with*
343 *chronic kidney disease.* Scientific Reports, 2017. **7**: p. 2870.
- 344 7. Meijers, B., et al., *Intestinal Barrier Function in Chronic Kidney Disease.* Toxins,
345 2018. **10**(7): p. 298.
- 346 8. Chen, G., et al., *Sodium Butyrate Inhibits Inflammation and Maintains Epithelium*
347 *Barrier Integrity in a TNBS-induced Inflammatory Bowel Disease Mice Model.*
348 *EBioMedicine*, 2018. **30**: p. 317-325.
- 349 9. Feng, W., et al., *Sodium Butyrate Attenuates Diarrhea in Weaned Piglets and*
350 *Promotes Tight Junction Protein Expression in Colon in a GPR109A-Dependent*
351 *Manner.* Cellular Physiology and Biochemistry, 2018. **47**(4): p. 1617-1629.
- 352 10. Snelson, M., M.T. Coughlan, and N.J. Kellow, *Modulation of the Gut Microbiota*
353 *by Resistant Starch as a Treatment of Chronic Kidney Diseases: Evidence of*
354 *Efficacy and Mechanistic Insights.* Advances in Nutrition 2019. **10**(2): p. 303-320.
- 355 11. Macia, L., et al., *Metabolite-sensing receptors GPR43 and GPR109A facilitate*
356 *dietary fibre-induced gut homeostasis through regulation of the inflammasome.*
357 *Nat Commun*, 2015. **6**.
- 358 12. Le Leu, R., et al., *Effect of high amylose maize starches on colonic fermentation*
359 *and apoptotic response to DNA-damage in the colon of rats.* Nutrition &
360 *Metabolism*, 2009. **6**(1): p. 1-9.
- 361 13. Cani, P.D., et al., *Changes in gut microbiota control inflammation in obese mice*
362 *through a mechanism involving GLP-2-driven improvement of gut permeability.*
363 *Gut*, 2009. **58**(8): p. 1091-1103.
- 364 14. Lancaster, G.I. and D.C. Henstridge, *Body Composition and Metabolic Caging*
365 *Analysis in High Fat Fed Mice.* JoVE, 2018(135): p. e57280.
- 366 15. Coughlan, M.T., et al., *Deficiency in Apoptosis-Inducing Factor Recapitulates*
367 *Chronic Kidney Disease via Aberrant Mitochondrial Homeostasis.* Diabetes,
368 2016. **65**(4): p. 1085-98.
- 369 16. Tan, J., et al., *Dietary Fiber and Bacterial SCFA Enhance Oral Tolerance and*
370 *Protect against Food Allergy through Diverse Cellular Pathways.* Cell Reports,
371 2016. **15**(12): p. 2809-2824.

- 372 17. Tan, J.K., et al., *Metabolite-Sensing G Protein–Coupled Receptors—Facilitators*
373 *of Diet-Related Immune Regulation*. Annual Review of Immunology, 2017. **35**(1):
374 p. 371-402.
- 375 18. Koh, G.Y., et al., *Dietary Resistant Starch Prevents Urinary Excretion of Vitamin*
376 *D Metabolites and Maintains Circulating 25-Hydroxycholecalciferol*
377 *Concentrations in Zucker Diabetic Fatty Rats*. The Journal of Nutrition, 2014.
378 **144**(11): p. 1667-1673.
- 379 19. Vaziri, N.D., et al., *High Amylose Resistant Starch Diet Ameliorates Oxidative*
380 *Stress, Inflammation, and Progression of Chronic Kidney Disease*. PLoS ONE,
381 2014. **9**(12): p. e114881.
- 382 20. Koh, G.Y., et al., *Consumption of Dietary Resistant Starch Partially Corrected the*
383 *Growth Pattern Despite Hyperglycemia and Compromised Kidney Function in*
384 *Streptozotocin-Induced Diabetic Rats*. Journal of Agricultural and Food
385 Chemistry, 2016. **64**(40): p. 7540-7545.
386

387

388

389

390

391

392

393

394 **Figure Legends**

395

396 **Figure 1: Intestinal Anatomy**

397 **A** Small intestine length, **B** Caecum length, **C** Colon length, **D** Small intestine weight, **E**
398 Caecum weight, **F** Colon weight. Data are expressed as mean \pm S.E.M. * $p < 0.05$, **
399 $p < 0.01$, *** $p < 0.001$, **** $p < 0.0001$. $n = 7-12$. WT = wildtype.

400

401 **Figure 2: Renal Injury and Inflammation**

402 **A** Urine albumin, **B** Blood urea nitrogen, **C** Relative kidney weight, **D** Plasma Cystatin
403 **C**, **E** Urinary MCP-1. Data are expressed as mean \pm S.E.M. * $p < 0.05$, **** $p < 0.0001$. $n =$
404 7-14. MCP-1 = Monocyte Chemoattractant Protein-1.

405

406 **Figure 3: Renal Structural Changes**

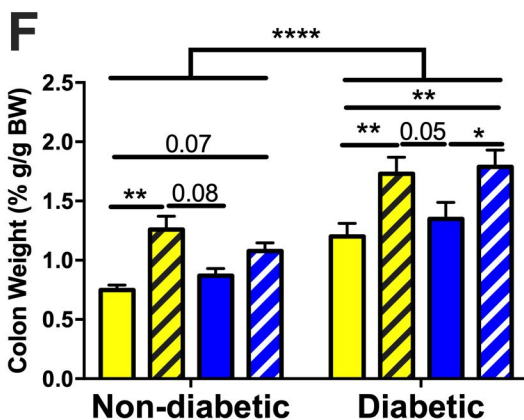
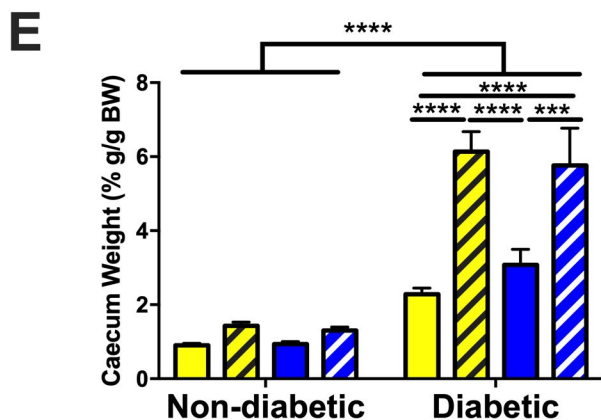
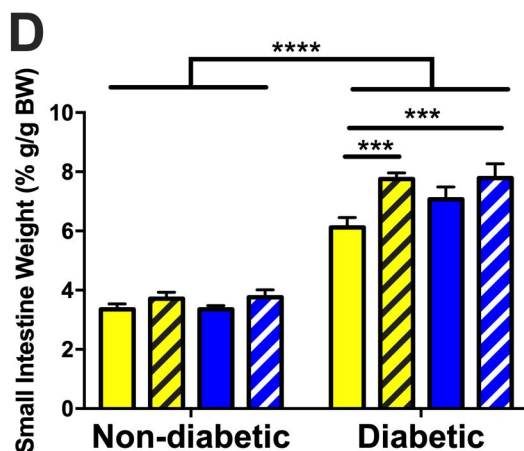
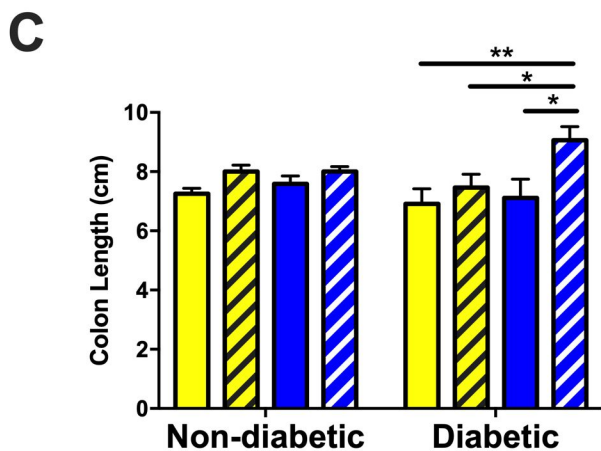
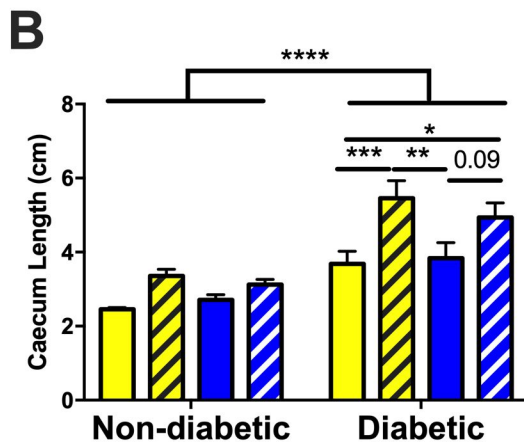
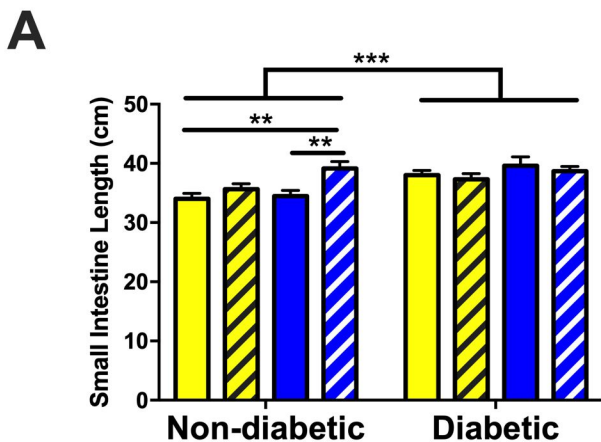
407 **A** Glomerulosclerotic Index Score, **B** Representative PAS stained images. Data are
408 expressed as mean \pm S.E.M. **** $p < 0.0001$. $n = 7-12$.

409

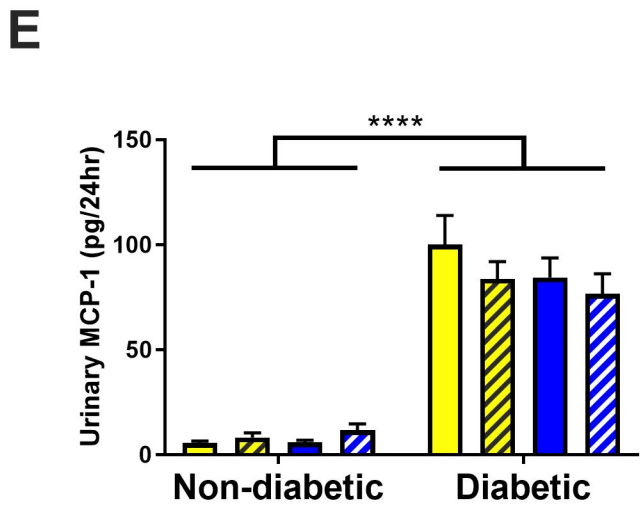
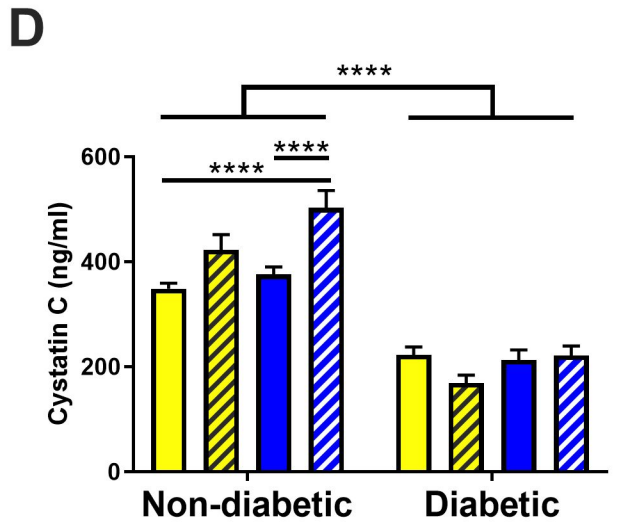
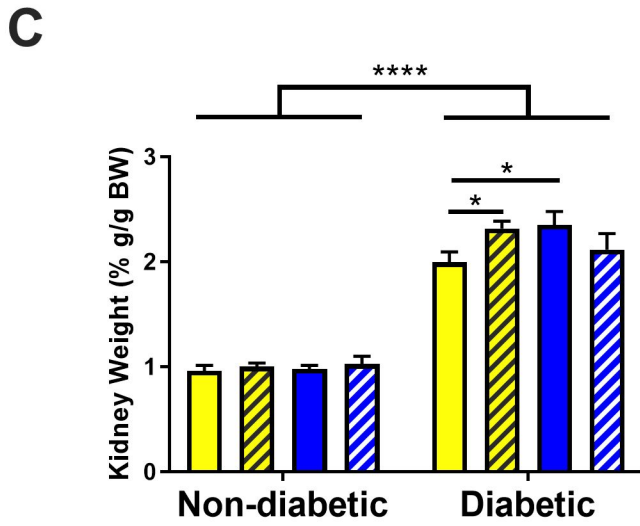
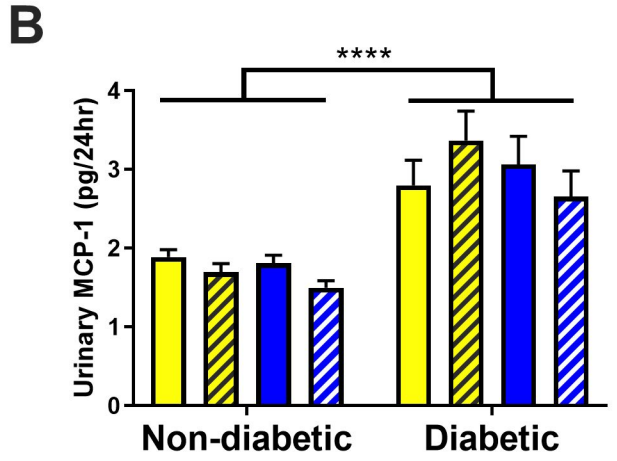
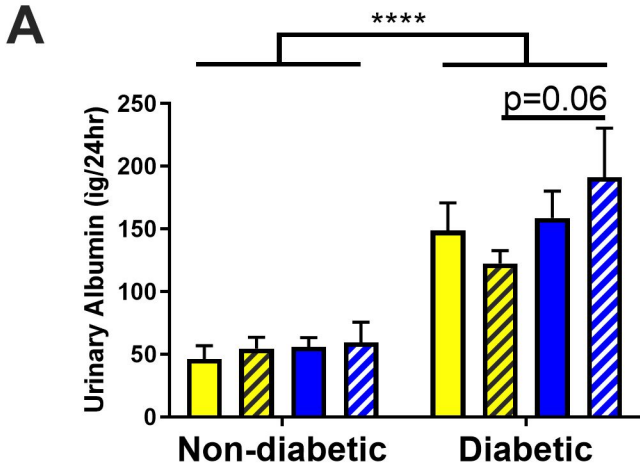
410 **Figure 4: Intestinal Permeability and Morphology**

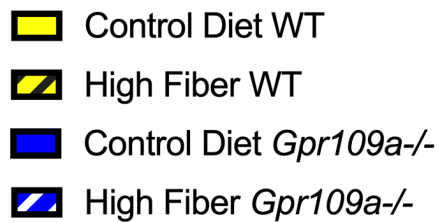
411 **A** Ileum villi height, **B** Ileum crypt depth, **C** Representative H&E stained images, **D**
412 Plasma dextran-FITC intestinal permeability assay, **E** Ileum expression of Occludin
413 (*Ocln*), **F** Ileum expression of Zonula occludens (*Tjp-1*). Data are expressed as mean \pm
414 S.E.M. *** $p < 0.001$, **** $p < 0.0001$. $n = 7-12$.

- Control Diet WT
- High Fiber WT
- Control Diet *Gpr109a*^{-/-}
- High Fiber *Gpr109a*^{-/-}

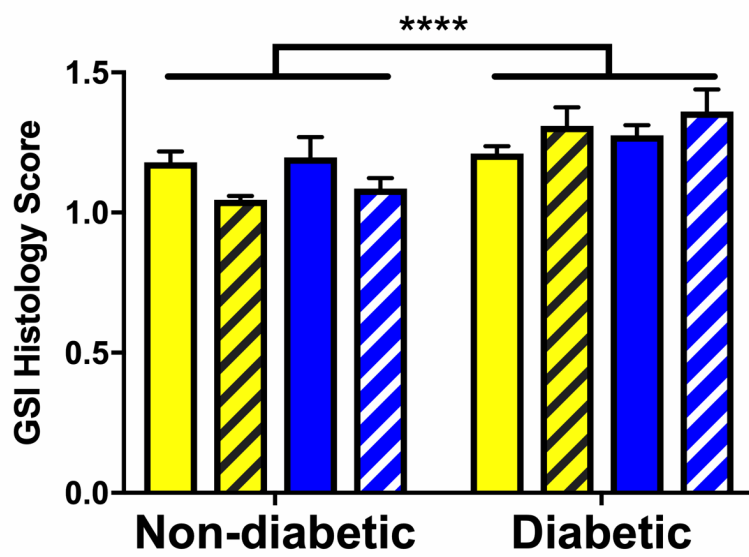


- Control Diet WT
- High Fiber WT
- Control Diet *Gpr109a*^{-/-}
- High Fiber *Gpr109a*^{-/-}

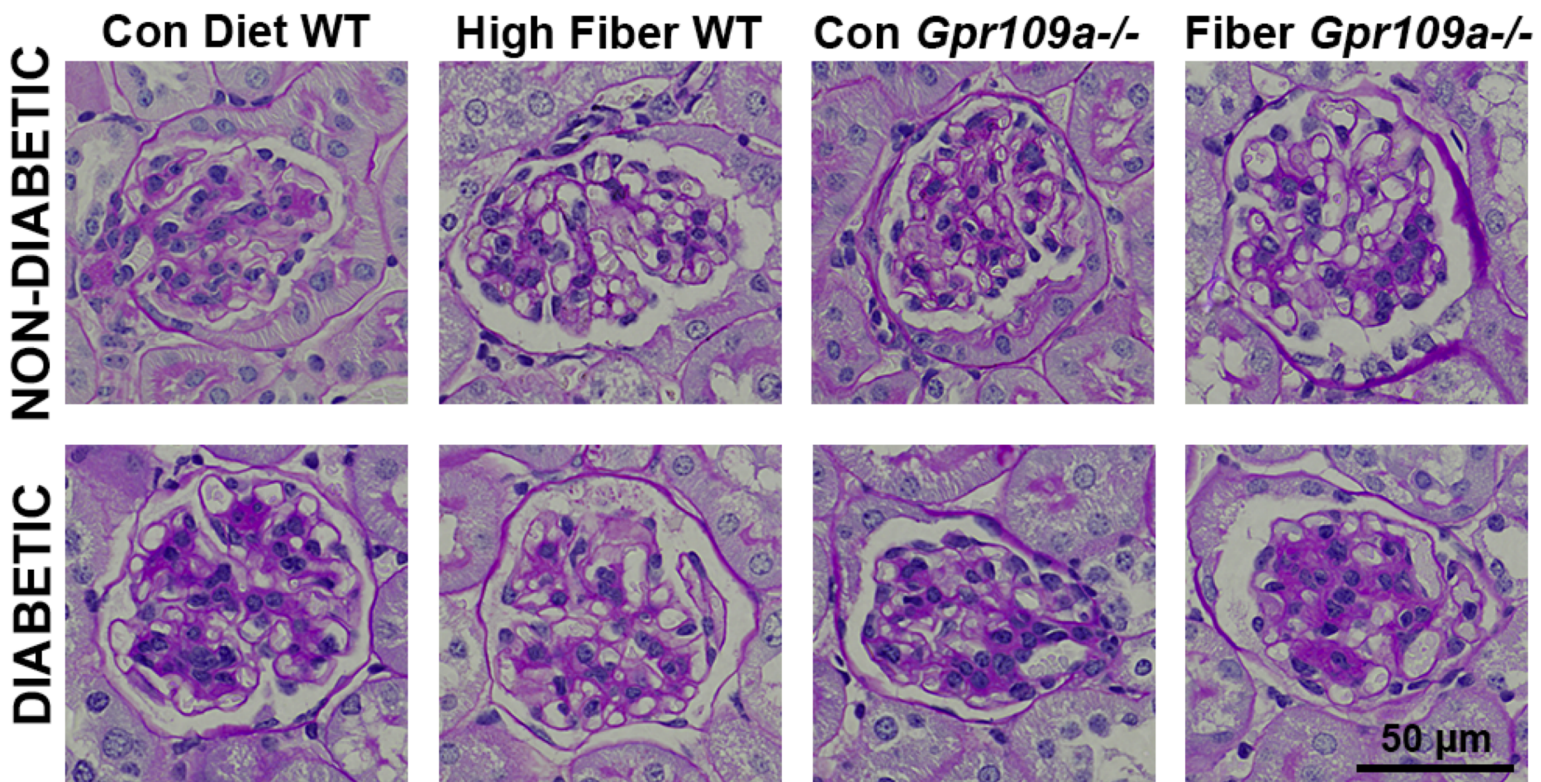




A



B



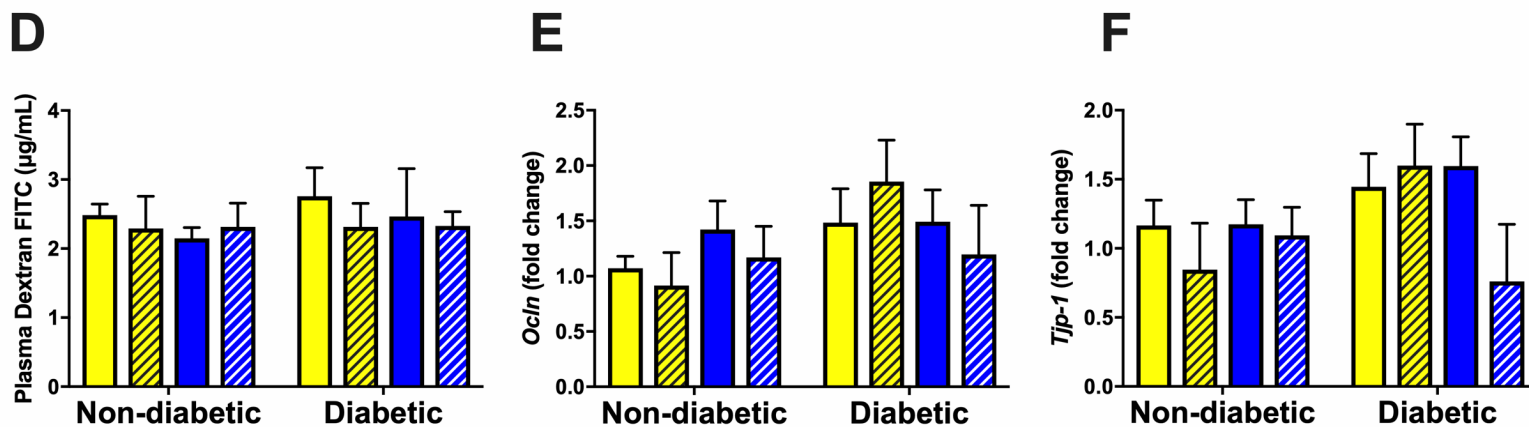
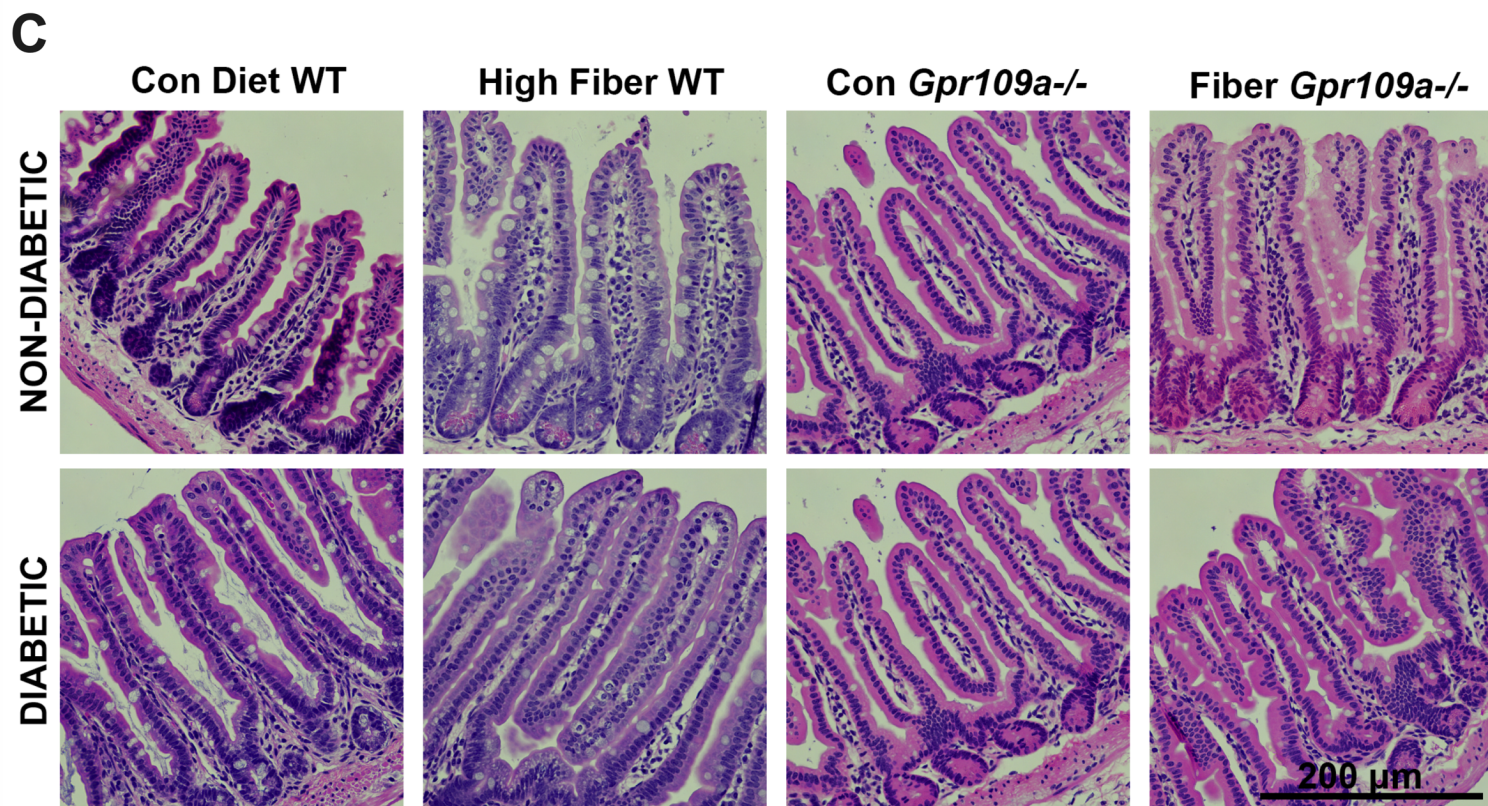
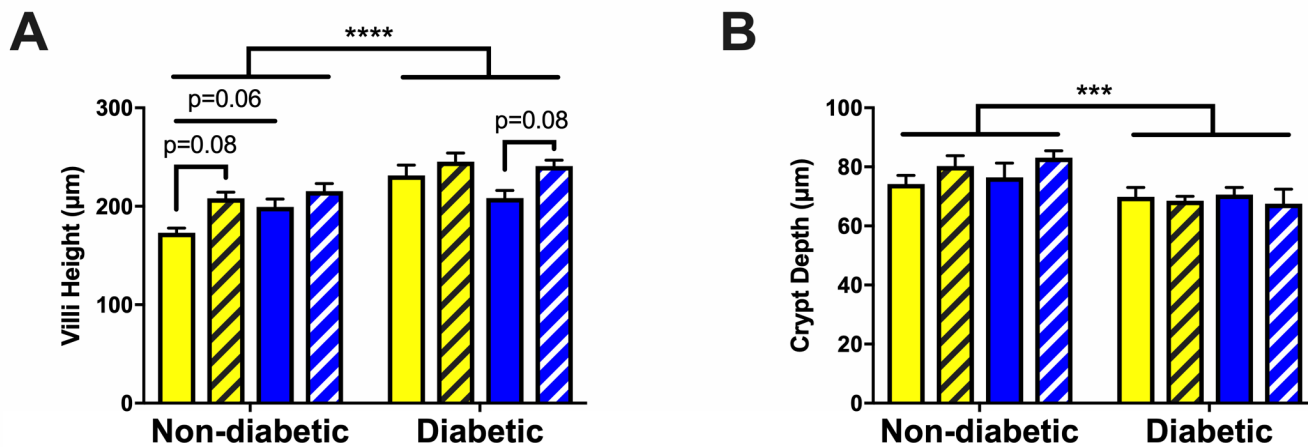
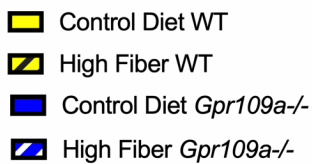


Table 1: Phenotypic and Biochemical Characteristics of Mice

	NON-DIABETIC				DIABETIC				Int	Genotype / Diet	Diab
	WT CON	WT HF	KO CON	KO HF	DIAB WT CON	DIAB WT HF	DIAB KO CON	DIAB KO HF			
Body weight (g)	35.6 ± 1.2	34.9 ± 1.6	37.7 ± 2.1	35.6 ± 1.4	24.3 ± 0.8	21.9 ± 0.6	22.3 ± 1.2	24.9 ± 1.0	NS	NS	****
GHb (%)	4.0 ± 0.0	4.3 ± 0.2	4.1 ± 0.1	4.0 ± 0.1	11.9 ± 0.5	12.3 ± 0.3	11.6 ± 0.5	11.8 ± 0.5	NS	NS	****
Fat Mass (%)	19.4 ± 1.7	19.5 ± 2.5	22.0 ± 1.7	20.7 ± 2.1	2.1 ± 0.5	1.4 ± 0.5	1.1 ± 0.5	1.0 ± 1.0	NS	NS	****
Lean Mass (%)	77.1 ± 1.6	77.0 ± 2.3	74.5 ± 1.7	75.8 ± 2.1	90.1 ± 0.5	90 ± 0.6	87.5 ± 0.7	89.7 ± 0.6	NS	NS	****
Urine Output	1.8 ± 0.2	2.0 ± 0.2	1.7 ± 0.1	1.8 ± 0.2	5.3 ± 0.3	5.6 ± 0.2	5.1 ± 0.3	4.8 ± 0.4	NS	NS	****
Water Intake	0.7 ± 0.1	1.0 ± 0.1	0.9 ± 0.1	1.0 ± 0.1	19.6 ± 2.2	18.7 ± 1.0	17.7 ± 2.0	16.4 ± 2.6	NS	NS	****
Liver (%)	3.9 ± 0.2	4.3 ± 0.2	4.4 ± 0.2	4.2 ± 0.2	5.4 ± 0.2	5.5 ± 0.2	6.0 ± 0.4	6.0 ± 0.4	NS	NS	****
Spleen (%)	0.3 ± 0.0	0.3 ± 0.0 ^a	0.3 ± 0.0	0.4 ± 0.1 ^a	0.3 ± 0.0	0.2 ± 0.0	0.3 ± 0.0	0.3 ± 0.0	NS	NS	*

Two-way ANOVA followed by Tukey's multiple comparisons test. Fat mass, lean mass, liver weight and spleen weight are expressed as % g/g body weight. Data are expressed as mean ± SEM, n= 7-14. * p<0.05, **** p<0.0001.

For post hoc test, cells within rows sharing the same superscript are significantly different from each other (^a)

p<0.05). GHb = Glycated Haemoglobin, CON = Control Diet, HF = High Fibre Diet, WT = wildtype, KO = knockout, Diab = diabetes, Int = interaction.